International Journal of Computational and Experimental Science and ENgineering (IJCESEN)

Vol. 11-No.1 (2025) pp. 1505-1514
http://www.ijcesen.com

ISSN: 2149-9144

Research Article

Production and Characterization of Electrical Conductive Polymeric Hybrid Composites Containing Organic and Inorganic Materials

Kutlay Sever[1*], Hüseyin Yılmaz[1], Metehan Atagür[2], İbrahim Şen[3]

[1]İzmir Katip Çelebi University, Mechanical Engineering Department, İzmir-TURKEY
* **Corresponding Author Email:** kutlay.sever@ikc.edu.tr- **ORCID:** 0000-0002-1606-8507

[1]İzmir Katip Çelebi University, Mechanical Engineering Department, İzmir-TURKEY
Email: hsynylmz90@gmail.com - **ORCID:** 0009-0003-6477-0274

[2]İzmir Katip Çelebi University, Metallurgical and Materials Engineering Department, İzmir-TURKEY
Email: metehan26mmz@gmail.com- **ORCID:** 0000-0002-1916-457X

[3]Bursa Technical University, Central Research Laboratory, Bursa-TURKEY
Email: ibrahim.sen@btu.edu.tr - **ORCID:** 0000-0003-2733-7191

Article Info:

DOI: 10.22399/ijcesen.242
Received : 24 November 2023
Accepted : 10 March 2025

Keywords :

Mica,
Carbon Nanotube,
Hybrid Composite.

Abstract:

Polymer composites are becoming more and more involved in many industries such as aerospace, automotive, transportation and sports. As usage increases in the commercial market, the polymer industry provides materials to almost every area of technology and industry, allowing the production of materials or new materials to be produced and the development or orientation of new types of needs. In the last 10 years, the use of polymer composites has become the new materials needed in electronic technology. The aim of this study is to investigate the effects of polypropylene (PP) on mechanical and conductivity properties by using mica (M) as an inorganic filler and carbon nano tube (CNT) as an organic filler. Before hybrid composite materials were produced, polypropylene (PP) and M-PP composites were produced and composite with the best mechanical properties were selected. PP-M composites were produced by using a thermokincetic mixer with the addition of mica in 10%, 20%, and 30% weight ratios. Hybrid composites were manufactured using CNT addition into PP-20M with %1, %3, %5, and %7 weight ratios. Mechanical properties of the composite materials produced using tensile and bending tests and viscoelastic properties by dynamic mechanical analysis (DMA), thermal properties by differential scanning calorimeter (DSC) and thermogravimetric (TGA) analyses and morphological structures by scanning electron microscopy (SEM) were investigated

1. Introduction

Polypropylene (PP) is the plastic raw material with the highest production, consumption, and trade in the world after polyethylene [1]. PP is a thermoplastic polymer with a low density (0.90-0.91 g/cm3) [2]. It is used in the production of products such as automotive parts, electronics, and kitchenware [3]. Reinforcements like as glass fiber, carbon fiber, and mica are used to enhance the properties of PP. The properties of PP can be improved depending on the type of reinforcement and chemical bonding [4]. Mica-filled polymers provide excellent surface qualities, as well as high thermal degradation, strength, hardness, and dimensional stability [5]. The addition of mica to a polymer can result in significant improvements to the material's properties, such as increasing tensile and flexural strengths, decreasing isotropic shrinkage and permeability, improving dielectric and thermal properties, and developing surface properties [6]. However, these composites are not electrically conductive. In recent years, theoretical and practical studies have focused on enhancing the electrical and thermal conductivity properties of polymers by using conductive filler or reinforcement material. Carbon black, carbon nanotubes, graphene, and graphene oxide are commonly used as carbon-based filler and reinforcing materials in the manufacture of conductive composites [7]. Antistatic materials can be used in medical devices, cables, transducers, and

gas sensors to protect from electromagnetic radiation and provide electrostatic discharge [8]. CNT is a nanomaterial with extremely unique mechanical, electrical and thermal properties. They can be incorporated into the polymer matrix to utilize the superior properties of CNTs such as electrical and thermal conductivity [9]. It has been observed that nanocomposites consisting of polymer matrices and carbon nanotubes have a great application potential for the electronics industry [10].

The effect of electrically conductive carbon nanotubes (CNT) and mica (M) as reinforcing materials on the mechanical, thermal, and electrical properties of polypropylene was investigated in this study. Mica (M)-PP composites were produced by mixing 10%, 20%, and 30% mica (M) with polypropylene (PP). Carbon nanotubes (CNT) were added to 20M-PP at rates of 1%, 3%, 5%, and 7% by weight while developing hybrid composite samples. The mechanical properties of the composite materials produced were tested using a universal testing device; their viscoelastic properties were discovered using a dynamic mechanical analyzer (DMA); their thermal properties were found using a differential scanning calorimeter (DSC) and thermogravimetric (TGA) analyzer; their electrical resistance was measured using a digital source meter; and their morphological structures were understood using a scanning electron microscope (SEM).

2. Material and Methods

2.1 Materials

Copolypropylene (PP) (LG Chemical PP M1500) was used as the polymer matrix. Micronized mica (SMW.125, D50=25 μm and density of 2.85 g/cm^3) used in composite was obtained from Kaltun Madencilik company and carbon nanotube (CNT) (KNT-MP industrial grade multi-walled carbon nanotube, BET surface area of 250-300 m^2/g, carbon purity >90%) was purchased from Graphene Chemical Industries (GCI). The diameter of the carbon nanotube is ~9.5 nm and the length are 1.5 μm.

2.2 Composite Production

A high-speed thermokinetic mixer (Gülnar Makine laboratory-type gelimat mixer, Turkey) was used to produce the composites. After adding different weight percentages of M and PP or M, CNT, and PP into the feeding chamber of the high-speed thermokinetic mixer, the entire material mixture was mixed at 2000 rpm for 20–30 seconds. After the mixing process was completed, the feeding chamber was immediately opened, and the molten mixture was taken with a wooden spatula and placed into a mold with dimensions of 150mmx150mmx1mm. It was hot-pressed for 5 minutes at 120 bar pressure and 190 °C using a temperature- and pressure-controlled hydraulic press (Gülnar Makina laboratory-type heated-cooled hydraulic press, Turkey). After the hot-pressing process, the samples were cold pressed under 120 bar pressure for 2 minutes. The sample codes of the produced composites and the PP, M, and CNT ratios in each composite are given in Table 1.

Table 1: *Composite sample codes and PP, M and CNT ratios in each composite*

Composite sample codes	PP (%)	M (%)	CNT (%)
PP	100	0	0
10 M-PP	90	10	0
20 M-PP	80	20	0
30 M-PP	70	30	0
PP20M-1CNT	79	20	1
PP20M-3CNT	77	20	3
PP20M-5CNT	75	20	5
PP20M-7CNT	73	20	7

2.3 Thermogravimetric Analyzes (TGA)

Thermal stability of the composites was determined by thermogravimetric analysis. Thermal properties of PP and its composites were analyzed with TA Instrument Q600 device. The samples were heated from room temperature to 600 ºC under nitrogen gas atmosphere at a rate of 10 ºC/min.

2.4 Differential Scanning Calorimetry (DSC) Analyses

DSC analyses were performed in a nitrogen gas atmosphere using the TA Instruments DSC Q2000 instrument to determine the thermal properties of PP and composites, including as melting and crystallization temperatures and melting and crystallization enthalpy values. To remove the samples' thermal history, they were heated from 20 ºC to 200 ºC at a rate of 10 ºC minute and then held at 200 ºC for 3 minutes. The samples were cooled to 20 ºC at a cooling rate of 10 ºC /minute, then heated to 200 ºC at a heating rate of 10 ºC /minute, and DSC data were obtained.

2.5 Mechanical Tests

Tensile tests were carried out with the use of a universal testing equipment equipped with a 5-kN load cell (Shimadzu Autograph AG-IS, Japan). The composites were tensile tested in accordance with

the ASTM D-638 standard, with the crosshead speed set to 50 mm/min. The flexural strength and modulus of the composites were evaluated using the three-point bending test in accordance with the ASTM D-790 standard. The three-point bending tests were performed on using a universal testing machine with a crosshead speed of 1 mm/min and a span length of 32 mm. To ensure repeatability, the tests were repeated at least three times for each type of composite.

2.5 Dynamic Mechanics Analysis (DMA)

A dynamic mechanical analysis (DMA) instrument (DMA Q800, TA instruments) was used to determine the storage modules and the tan delta properties of the composites. The instrument was tested with a single cantilever at temperatures ranging from 40 to 135 ºC with a heating rate of 3 ºC /minute.

2.6 Electrical Resistivity Measurements

Surface resistivities of PP, M-PP, and PP-M-CNT composite plates were measured with a Keithley Digital Sourcemeter according to the ASTM D257 method.

2.7 Scanning Electron Microscopy Observation

The fracture surfaces of the composites were observed using a scanning electron microscope (SEM) (Carl Zeiss 300VP, Germany) operated at 2.5 kV. A thin layer of gold was coated on the fractured surface of the composites by using an automatic sputter coater (Emitech K550X) to reduce the extent of sample arcing during SEM observation.

3. Results and Discussions

3.1 Thermogravimetric Analysis (TGA)

TGA analysis was used to investigate the thermal degradation behavior of PP, M-PP, and PP-M-CNT composites. TGA curves were used to calculate the onset and maximum thermal degradation temperatures. Figures 1 and 2 show the thermal degradation behaviors of composites. Pure PP starts its thermal degradation at 413.72 °C, as seen in Table 2. Once M particles are added to pure PP, the temperature rises. The 30M-PP composite had the highest onset degradation temperature. This is due to the barrier effect of mica against thermal degradation, and the barrier effect absorbs energy and temperature within the material [11]. Table 2 shows that the maximum degradation temperature of pure PP is 457.37 °C. The maximum

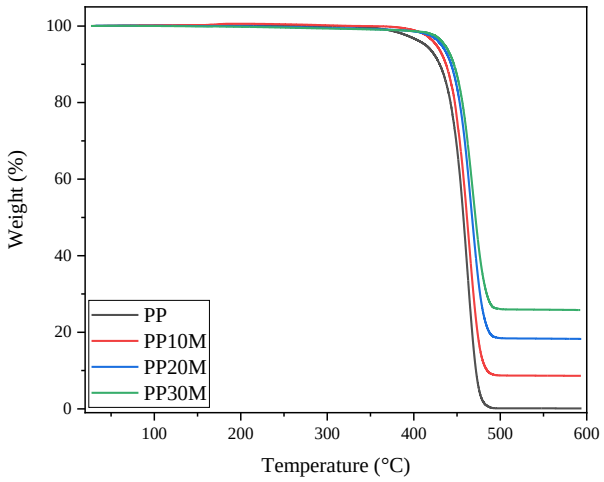

Figure 1. *TGA curves of PP and M-PP composites.*

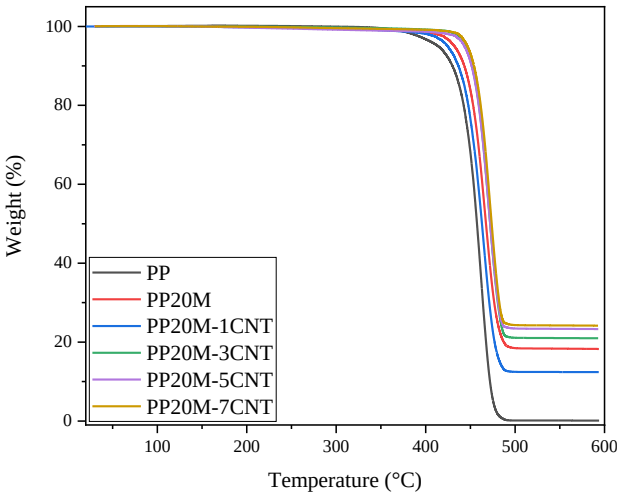

Figure 2. *TGA curves of PP, 20M-PP and PP-M-CNT composites.*

thermal degradation temperature of the PP increased as the M concentration in PP increased. The 30M-PP composite had the highest maximum degradation temperature among M-PP composites, with a value of 471.35 °C. This is because mica has a high interface interaction [12]. Except for the PP20M-1CNT hybrid composite, the onset and maximum degradation temperatures of the hybrid composites increased compared to 20M-PP. The highest onset and maximum degradation temperatures were detected in the PP20M-7CNT hybrid composite, and the onset and maximum degradation temperature values for this composite are 446.78°C and 473.84°C, respectively. The reason for this increase is that the nanotubes incorporated into the polymer matrix allow heat to spread uniformly throughout the composite. As a result, thermal degradation temperature values increased with the increase in the CNT ratio. In addition, the conductivity of CNTs and the better energy transfer between bonds increased these

Table 2: *TGA data of PP, M-PP and PP-M-CNT composites*

Sample Code	ODT (°C)	MDT (°C)	EDT (°C)	ML (%)
P	413.72	457.37	489.97	99.77
10M-PP	425.85	461.48	491.04	91.10
20M-PP	432.08	467.45	492.23	81.68
30M-PP	435.88	471.34	498.96	70.05
PP20M-1CNT	424.60	462.94	493.28	87.80
PP20M-3CNT	444.64	472.10	492.22	78.87
PP20M-5CNT	443.20	472.09	496.26	76.57
PP20M-7CNT	446.78	473.84	499.50	75.72

** Onset Degradation Temperature: ODT, Maximum Degradation Temperature: MDT, End Degradation Temperature: EDT, Mass Loss: WL.*

temperature values as the amount of CNTs increased [13]. Since nanotubes have good thermal conductivity, heat applied to the composites can be easily dissipated [14].

3.2 Differential Scanning Calorimetry (DSC)

The DSC curves of pure PP, M-PP, and M-CNT composites are shown in Figures 3 and 4.

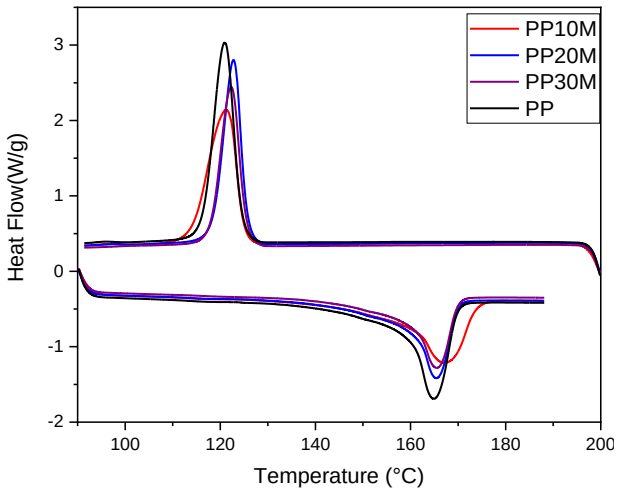

Figure 3: *DSC graphs of PP and M-PP composites.*

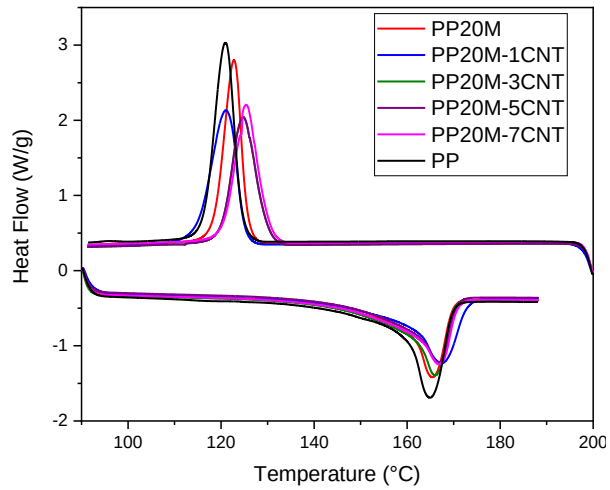

Figure 4. *DSC graphs of 20M-PP and PP20M-CNT composites.*

Table 3 exhibits the Tm (melting temperature), Tc (crystallization temperature), Hm (melting enthalpy), Hc (crystallization enthalpy), and Xc (degree of crystallinity) values of PP, M-PP, and PP-M-CNT composites.

Degree of crystallinity for M-PP and M-CNT-PP composites;

$$Xc(\%) = \frac{\Delta H_m / \Phi_{PP}}{\Delta H_m^{\circ}} * 100 \qquad (1)$$

Equation 1 was used to calculate the Xc values. The expressions in the formula are as follows: H°m=melting enthalpy of 100% crystal PP, ϕpp=weight percentage of PP in the composite. The melting enthalpy of 100% crystalline PP was assumed to be 209 J/g in the Xc calculation [15]. As indicated in Table 3, M particles added to PP had a weak effect on the melting temperature. It is believed that the crystal size of PP does not change visibly with M particles [16]. The Tc value of PP is lower than the Tc value of the M-PP composite. With the addition of M, the Tc value increased by an average of 1.29–2.28 °C. Additionally, when the Tc value of the 20M-PP composite is compared with the Tc values of the PP-M-CNT hybrid composites, an increase of 1.04–5.40 °C is observed on average. The reason for this increase is thought to be the nucleation effect of CNTs [17]. When the Tm values of hybrid composites were compared to the 20M-PP composite, as illustrated in Figure 4, it was found that the effect of CNT on Tm of PP was lower. It is an indication that CNT does not change the crystal sizes of polymers [18]. The Tc values of PP-M-CNT hybrid composites are higher than the Tc values of PP. In addition, when 20M-PP composites are compared to hybrid composites, the Tc value of hybrid composites is 2.5°C higher on average. The reason for this increase can be explained by the heterogeneous nucleation effect of CNTs [19]. While the Xc value of 20M-PP composite is 1.62% higher than the Xc value of PP, the Xc value of PP20M-7CNT composite is 3.49% higher than the Xc value of PP. With this result, it is thought that CNT particles are not very effective in increasing the crystallinity degree of PP.

3.3. Mechanical Tests

Mechanical properties such as tensile strength, Young's modulus, flexural strength, and flexural modulus of PP, M-PP composites, and PP-M-CNT hybrid composites are given in Table 4. Variations in the tensile strength and Young's

Table 3: *Tm, Tc, ΔHm, ΔHc, and Xc values of PP, M-PP and PP-M-CNT composites.*

Sample codes	Tm (°C)	Tc (°C)	ΔH_c (j/g)	ΔH_m (j/g)	Xc (%)
PP	164.9	120.9	86.9	81.0	38.8
10M-PP	167.2	121.3	77.9	77.4	41.1
20M-PP	165.4	122.8	69.8	67.5	40.4
30M-PP	165.5	122.3	63.3	60.2	41.2
PP20M-1CNT	167.3	121.0	73.3	64.0	38.9
PP20M-3CNT	166.0	124.8	70.6	63.8	39.7
PP20M-5CNT	166.7	124.7	66.3	61.1	39.0
PP20M-7CNT	166.9	125.4	68.9	63.8	41.8

Tablo 4: *Mechanical properties of PP, M-PP and M-CNT-PP composites*

Sample Code	Tensile Strength (MPa)	Young's Modulus (MPa)	Flexural Strength (MPa)	Flexural Modulus (MPa)
PP	22.3	925.1	35.	1042.6
10M-PP	21.4	1125.3	37.1	1284.8
20M-PP	21.5	1295.7	36.4	1490.7
30M-PP	21.3	1461.7	35.0	1597.5
PP20M-1CNT	22.0	1254.4	40.5	1361.5
PP20M-3CNT	21.3	1333.5	39.4	1321.9
PP20M-5CNT	21.6	1376.7	35.3	1249.2
PP20M-7CNT	21.5	1503.6	32.7	1228.5

modulus of PP and M-PP composites and PP-M-CNT hybrid composites are shown in Figure 5 and 6. As seen in Table 4, the tensile strength of PP is 22.3 MPa. A decrease in the tensile strength of PP was observed with the addition of M to PP. However, as the M ratio added to PP increased, no significant decrease in tensile strength was observed. The reason for the decrease in tensile strength is that, due to mica's lamellar structure, the materials are not mixed at sufficient temperature and time in composite production.

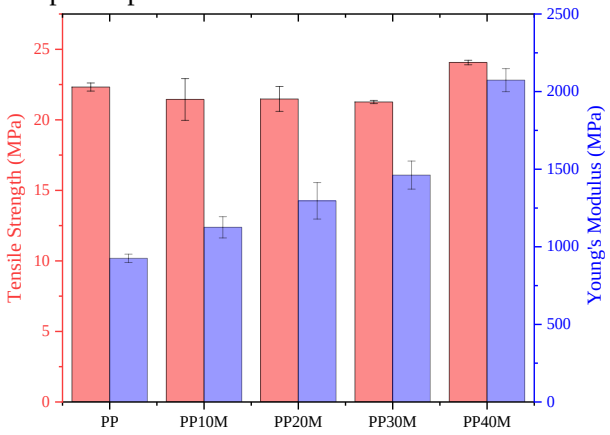

Figure 5. *Variations in tensile strength and Young's modulus of M-PP composites.*

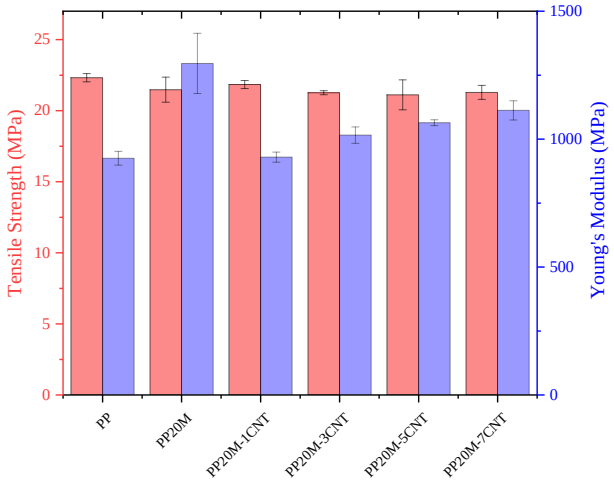

Figure 6. *Variations in tensile strength and Young's modulus of M-PP-CNT composites.*

As a result, mica is not distributed homogeneously within the matrix structure [20]. The tensile strength of PP-M-CNT hybrid composites is lower than PP. The tensile strength of the composites almost did not change with the addition of carbon nanotubes. Only a slight increase in the tensile strength of the PP20M-1CNT hybrid composite was observed. The reasons for not increasing the tensile strength are that as the number of particles increases, the distribution of the particles in the matrix is not homogeneous, and the interfacial adhesion of the matrix and particles is weak [21]. CNTs include atomically smooth non-reactive surfaces, limiting load transfer due to insufficient interfacial interaction between the CNT and the polymer chains. As a result, the benefits of CNTs' strong mechanical characteristics are underused [22]. Young's modulus of PP is 925.1 MPa. An increase in the Young's modulus was detected with the addition of M to the PP matrix. The highest Young's modulus value was seen in the 30M-PP composite, and this value was 1461.7 MPa. The Young's modulus of the composite formed by adding 30% M is 63% higher than the Young's modulus of pure PP. The reason for the increase in the Young's modulus with the addition of mica is that the stiffness of the M particles is higher than that of the PP matrix [23]. The changes in the Young's modulus of PP and PP-M-CNT composites are shown in Figure 6. Compared to Young's modulus of the 20M-PP composite, Young's modulus of hybrid composites with CNT added increased, except for the composite with the PP20M-1CNT ratio. The reason for this is thought to be that PP has a lower Young's modulus than CNT. Variations in the flexural strength and flexural modulus of PP and M-PP composites are shown in Figure 7. Figure 8 illustrates changes in the flexural strength and flexural modulus of PP, PP-20M and PP-M-CNT composites.

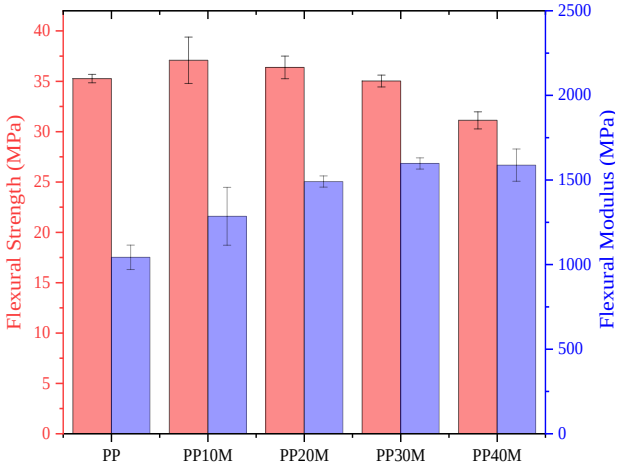

Figure 7. *Variations in flexural strength and flexural modulus of M-PP composites.*

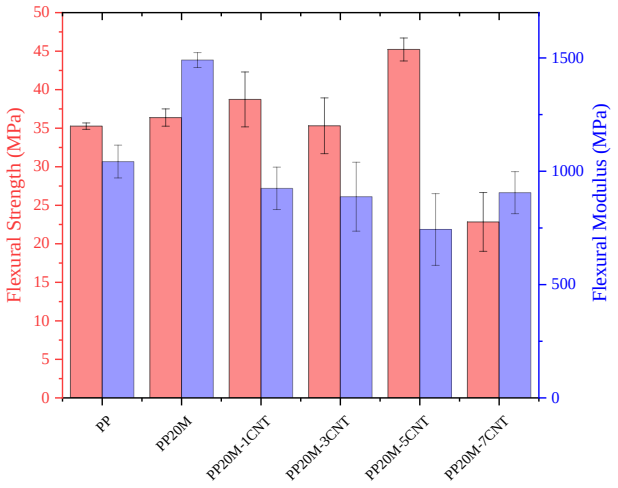

Figure 8. *Variations in flexural strength and flexural modulus of M-PP-CNT composites.*

The flexural strength of PP is 35.3 MPa. An increase in the flexural strength of PP was observed by adding 10% M particles to PP. The reason for this increase is the more homogeneous distribution of mica added to PP at low rates [24]. As the more M ratio added to PP increased, a decrease in flexural strength was detected compared to 10M-PP. Incorporating high amounts of M particles into PP may prevent the homogeneous mixing of mica in the PP and cause agglomeration. Additionally, the flexural strength of the composites may have decreased due to the irregularly shaped M particles not supporting the stresses transferred from the matrix [24]. The flexural strength of the PP-20M-1CNT hybrid composite is highest among the hybrid composites. The PP-20M-1CNT composite has a flexural strength of 40.5 MPa, which is 11.32% higher than the flexural strength of 20M-PP. A more homogenous distribution or less agglomeration may have resulted from the addition of 1% CNT to 20M-PP. Flexural strength was reduced when more than 1% CNT was incorporated to 20M-PP. The main reason for this may be that agglomerations occur more often in polymers with high CNT ratios. The flexural strength of PP-M-CNT hybrid composites, on the other hand, is higher than that of 20M-PP and pure PP. The flexural modulus of PP is 1042.6 MPa. An increase in the flexural modulus was determined with the addition of M particles into PP. 30M-PP composite is the composite with the highest flexural modulus and its flexural modulus was found to be 1597.5 MPa. The flexural modulus of 30M-PP composite is 65% higher than the flexural modulus of PP. The reason for this increase is that M particles are more rigid than PP. The moduli of mineral particles are much higher than those of the polymer matrix [25]. When hard-structured filler materials are introduced to thermoplastics, the flexural modulus is expected to increase [26]. The addition of CNT to the 20M-PP composite resulted in a reduction in the composite's flexural modulus. Agglomerations in hybrid composites may have led to a decrease in flexural modulus. Because the agglomerations prevent the homogenous distribution of the material in the composite and the load distribution is not uniformly distributed [27].

3.4. Dynamic mechanics analysis (DMA)

Figures 9 and 10 indicate the storage modulus and tan delta variations of PP, M-PP and PP-M-CNT composites as a function of temperature. The storage modulus of PP is lower than the storage modulus values of M-PP composites. The storage modulus of M-PP composites increased as the M ratio added to PP increased. The 30M-PP composite had the highest storage modulus among M-PP composites. The storage modulus of the 30M-PP composite is 63.50% higher than that of PP at 35°C. This is because PP has a lower mechanical strength than mica [28]. Furthermore, Figure 9 shows that the storage modulus of all M-PP composites decreases as temperature increases. As seen in Figure 10, the storage modulus of all hybrid composites reduces as temperature rises. The decrease in storage modulus with increasing temperatures is due to the beginning of the relaxation process in the polymer, softening of the materials, and an increase in the molecular mobility of the polymer chains [29]. Figure 11 shows Tan delta changes of PP and M-PP composites depending on temperature, and no significant increase was observed in the Tan delta peak values of M-PP composites. Among M-PP composites, 10M-PP composite has the lowest Tan delta peak value. Tan delta values for all hybrid composites are shown in Figure 12. The tan delta peak height decreased with the addition of CNTs due

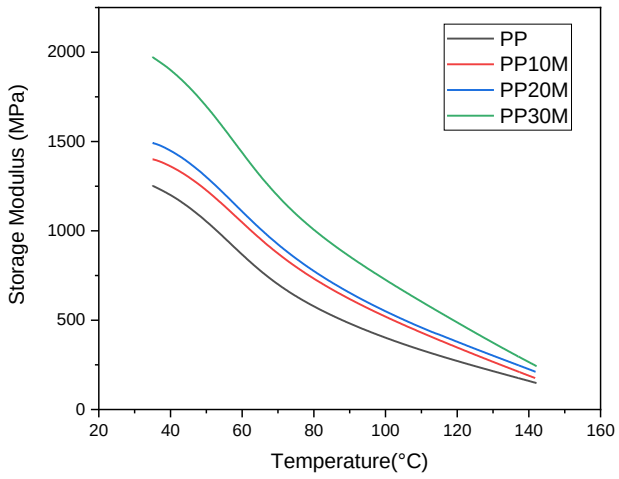

***Figure 9**: Variations in the storage modulus of PP and M-PP composites depending on temperature.*

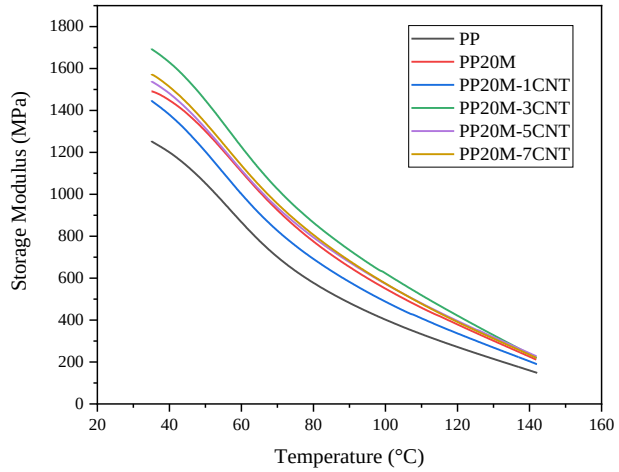

***Figure 10:** Variations in the storage modulus of PP, 20M-PP and PP-20M-CNT composites depending on temperature.*

to the inhibition of the movement of the interfacial molecular chains [30]. The PP-20M-1CNT composite has the lowest Tan delta value among PP-M-CNT hybrid composites. Tan delta can be utilized to collect information about the interface properties formed between the reinforcing material and the polymer matrix [31]. A considerably stronger interface is defined by lower usage of energy and a low tan delta peak intensity [32]. The tan delta indicates energy dissipation of material, and a lower tan delta peak suggests better interfacial bonding between the CNTs and the matrix [33].

3.5. Electrical Resistance Measurement

The surface resistivity values of PP, M-PP, and PP-M-CNT composites are shown in Figures 13 and 14. Electrical conductivity is inversely proportional to surface resistivity. It can be said that electrical conductivity increases as electrical resistivity

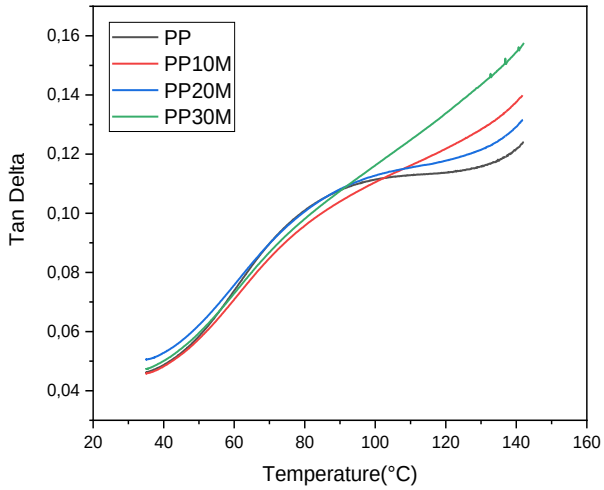

***Figure 11:** Tan Delta changes of PP and M-PP composites depending on temperature.*

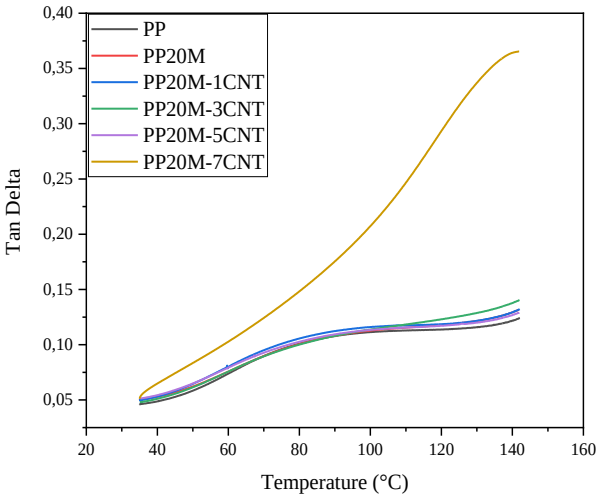

Figure 12: Tan Delta changes of PP, 20M-PP and hybrid composites depending on temperature.

decreases [34]. The surface resistivity of pure PP was found to be $1.00x10^{-16}$. A slight change in surface resistivity was observed with the addition of mica particles to PP. The highest surface resistivity value was determined in the 30M-PP composite, and this value is $2.04\ x10^{-16}$. This is two times higher than the surface resistivity value of PP. The reason for this increase is due to the acidic properties of mica minerals [34].

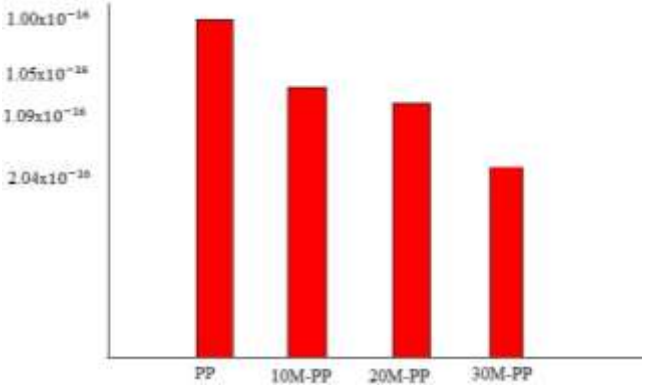

***Figure 13:** Variation in surface resistivity of PP and M-PP composites*

One of the most important properties of CNTs is its high electrical conductivity [35]. When 1% CNT is added to the PP matrix, the surface resistivity of PP starts to reduce. As the CNT ratio added to PP increased, the surface resistivity gradually decreased. As a result, an increase in electrical conductivity was observed. The PP20M-7CNT hybrid composite had the lowest surface resistivity among the hybrid composites, with an electrical resistivity value of 8.80 x10^{-7}. As the CNT content increases, the electrical resistance in composites decreases, and a conductive chain network begins to form in composites containing CNT [36].

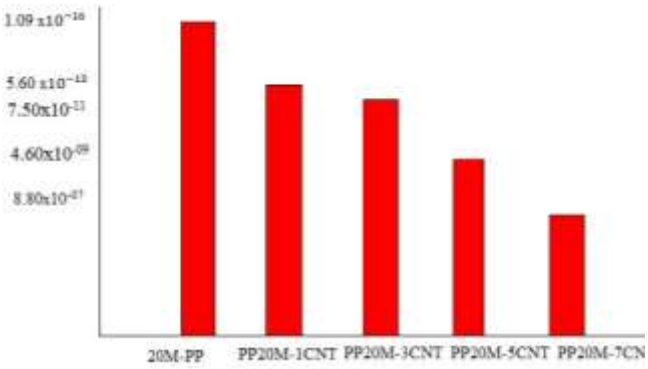

Figure 14: *Variation in surface resistivity of 20M-PP and its hybrid composites*

3.4. Scanning Electron Microscope (SEM) Observations

As seen in Figures 15 and 16, SEM images were taken from the broken surfaces of the composite samples because of the tensile test. It has been observed that as the mica ratio in the composites increases, the fracture behavior gradually changes from ductility to brittleness. The reason why the composite shows such fracture behavior with M may be due to the brittle fracture due to the lamellar structure of mica. In M-PP composites, as the M ratio increased, the particles agglomerated and pulled out. The reason for this is thought to be that as the mica value increases, the interface interaction decreases. CNTs are difficult to separate from each other in the polymer matrix due to their poor dispersion, i.e. agglomerations [37]. As a result, as the CNT ratio in the hybrid composites generated increases, CNTs may form agglomerates and may not be dispersed uniformly throughout the composite. SEM examination clearly shows an accumulation of nanotubes in groups in the composite in Figure 16. CNT agglomerations can be seen as particles ranging in size from 0.5 to 20 µm [38]. As the CNT ratio increases, the size of these visible particles (agglomerated CNTs) increases. In hybrid composites with a lower CNT ratio, this size is between 0.2 and 10 µm [39].

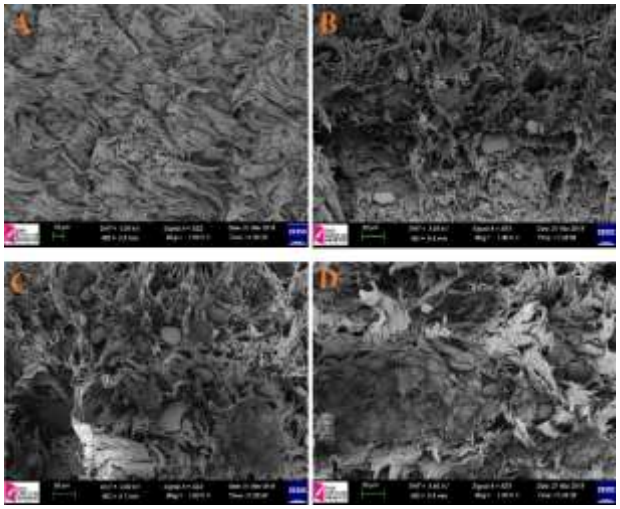

Figure 15: *SEM images of A) PP, B) 10M-PP, C) 20M-PP, D) 30M-PP composites*

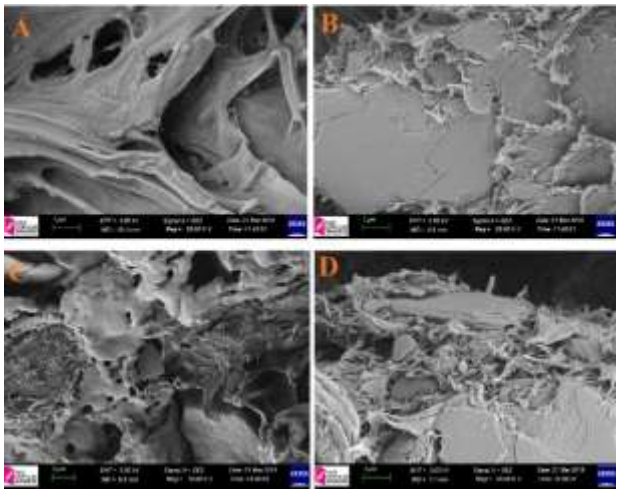

Figure 16: *SEM images of PP20M-1CNT, PP20M-3CNT, PP20M-5CNT, PP20M-7CNT hybrid composites*

5. Conclusion

PP matrix composites were produced using mica and CNT, and the mechanical, thermal, and electrical properties of the composites were examined. An increase in the onset and maximum decomposition temperatures of PP was observed with the addition of M to PP. Among M-PP composites, the maximum degradation temperature was seen in the 30M-PP composite, and its value is 471.34 °C. By adding CNT to the 20M-PP composite (except PP20M-1CNT), an increase in the onset and maximum decomposition temperatures was observed, and the highest onset and maximum decomposition temperatures were detected in the PP20M-7CNT composite. The Young's modulus of PP is 925.07 MPa. An increase in the Young's modulus was detected with the addition of M to the PP matrix. The highest Young's modulus value was seen in the 30M-PP composite, and this value was 1461.70 MPa. The Young's modulus of the composite

formed by adding 30% M is 58% higher than the Young's modulus of pure PP. Compared to the Young's modulus of the 20M-PP composite, the Young's modulus of hybrid composites with CNT added increased, except for the composite with the PP20M-1CNT ratio. The highest Young's modulus value was seen in the 20M-PP-7CNT composite, and this value was 1503.63 MPa. The Young's modulus of the 20M-PP-7CNT composite formed by adding 20%M and 7% CNT is 62.54% higher than the Young's modulus of pure PP. The storage modulus of M-PP composites increased as the M ratio added to PP increased. The 30M-PP composite had the highest storage modulus among M-PP composites. The storage modulus of the 30M-PP composite is 63.50% higher than that of PP at 35°C. The storage modulus of the PP-20M-3CNT composite is 44.07 % and 21.18% higher than that of PP and 20M-PP at 35°C, respectively. With the addition of M to PP, a slight change was observed in its electrical resistivity. A significant decrease was observed in the electrical resistivity values of the hybrid composites created by CNT on the 20M-PP composite. The lowest electrical resistivity value was examined in the PP20M-7CNT composite, and its value is 8.80 x10^{-7}.

Author Statements:

- **Ethical approval:** The conducted research is not related to either human or animal use.
- **Conflict of interest:** The authors declare that they have no known competing financial interests or personal relationships that could have appeared to influence the work reported in this paper
- **Acknowledgement:** The authors declare that they have nobody or no-company to acknowledge.
- **Author contributions:** The authors declare that they have equal right on this paper.
- **Funding information:** The authors declare that there is no funding to be acknowledged.
- **Data availability statement:** The data that support the findings of this study are available on request from the corresponding author. The data are not publicly available due to privacy or ethical restrictions.

References

[1] Polipropilen, S.T.A Plastik San. Ve Tic.Ltd. Şti. Raporu.

[2] Metin,D.(2002). Interfacial enhancement of polypropylene-zeolite composites *(Master's thesis, Izmir Institute of Technology)*.

[3] Dünya ve Türkiye polipropilen (PP) raporu. 2015-*PEGEV*.(2015).

[4] Wright, T., Bechtold, T., Bernhard, A., Manian, A. P., & Scheiderbauer, M. (2019). Tailored fibre placement of carbon fibre rovings for reinforced polypropylene composite part 1: PP infusion of carbon reinforcement. *Composites Part B: Engineering*, 162, 703-711.

[5] Ferro, P. J., & Stevard, H. W. (1987). Mica-a summary of 1986 activity: *Mining Engineering.*

[6] Sarah Whipkey, Chance Roman, and Kevin Seay.(2015). Processing and Characterization Techniques for a Mica Filled Polymer Composite. *Journal of Undergraduate Materials Research*, 5.

[7] Topal, E., (2014). Kompozit Delikli Kare Levhalarda İki Yönlü Yükleme Altinda Mekanik Burkulmalarinin İncelenmesi. *MSc Thesis Hitit University*

[8] Vinay H, B., Govindaraju, H., & Banakar, P. (2015). PROCESSING AND CHARACTERIZATION OF GLASS FIBER AND CARBON FIBER REINFORCED VINYL ESTER BASED COMPOSITES. *International Journal of Research in Engineering and Technology*, 04, 401-406.

[9] Stewart,K. (2009) & Stewart, R. (2009). Carbon fibre composites poised for dramatic growth, *Reinforced Plastics*,53.

[10] Bishui,B.M., Dar,R.N. & Mandel,S.S. (1961). Studies on Indian Mica; Effects on Dry Ground on DTA, Control Glass and Ceram., *Research Inst. Bui*, 8(1), 15-22.

[11] Sever, K., Atagür M., Tunçalp, M., Altay, L., Seki Y., & Sarıkanat, M. (2018). The Effect of Pumice Powder on Mechanical and Thermal Properties of Polypropylene, *Journal of Thermoplastic Composite*, DOI: 10.1177/0892705718785692.

[12] Romanzini, D., Ornaghi Jr, H. L., Amico, S. C., & Zattera, A. J. (2012). Influence of fiber hybridization on the dynamic mechanical properties of glass/ramie fiber-reinforced polyester composites. *Journal of Reinforced Plastics and Composites*, 31(23), 1652-1661.

[13] Yang, J., Lin, Y., Wang, J., Lai, M., Li, J., Liu, J., ... & Cheng, H. (2005). Morphology, thermal stability, and dynamic mechanical properties of atactic polypropylene/carbon nanotube composites. *Journal of Applied Polymer Science*, 98(3), 1087-1091.

[14] Seo, M. K., & Park, S. J. (2004). A Kinetic Study on the Thermal Degradation of Multi- Walled Carbon Nanotubes- Reinforced Poly (propylene) Composites. *Macromolecular Materials and Engineering*, 289(4), 368-374.

[15] Bikiaris, D. (2010). Microstructure and properties of polypropylene/carbon nanotube nanocomposites. *Materials*, 3(4), 2884.

[16] Manchado, M. L., Valentini, L., Biagiotti, J., & Kenny, J. M. (2005). Thermal and mechanical properties of single-walled carbon nanotubes–polypropylene composites prepared by melt processing. *Carbon*, 43(7), 1499-1505.

[17] Kaya, N., Atagur, M., Akyuz, O., Seki, Y., Sarikanat, M., Sutcu, M., ... & Sever, K. (2018). Fabrication

and characterization of olive pomace filled PP composites. *Composites Part B: Engineering*, 150, 277-283.

[18] Yang, B. X., Shi, J. H., Pramoda, K. P., & Goh, S. H. (2008). Enhancement of the mechanical properties of polypropylene using polypropylene-grafted multiwalled carbon nanotubes. *Composites Science and Technology*, 68(12), 2490-2497.

[19] Xu, D., & Wang, Z. (2008). Role of multi-wall carbon nanotube network in composites to crystallization of isotactic polypropylene matrix. *Polymer*, 49(1), 330-338.

[20] Putnam, J. W., & Watson, C. R. (2002). U.S. Patent No. 6,334,617. Washington, DC: *U.S. Patent and Trademark Office.*

[21] Shuming, D.,Tarosava, E., Krumme, A., & Meier, P.(2011). Rheological and mechenical properties of poly(lactic) acid/ cellulose and LDPE/cellulose composites. *Materials Science*, 17(1), 32-37.

[22]Choudhary, B.P. Singh and R.B. (2013) Mathur Syntheses and Applications of Carbon Nanotubes and Their Composites, *Edited by Satoru Suzuki, Carbon Nanotubes and Their Composites*, DOI: 10.5772/52897

[23] Okuno,K.,& Woodhams, R. T. (1975). Mica reinforced polypropylene. *Polymer Engineering & Science*, 15(4), 308-315.

[24] Reyes, J. E. P. (2015). Effect of surface treatment and particle loading on the mechanical properties of CFB fly ash reinforced thermoset composite. *International Journal of Chemical Engineering and Applications*, 6(1), 6.

[25]-Sabu,T.,&Pothan,L.(2008).-Cellulose fibre reinforced polymer composites. *Philadel-phia: Old City Publishing*.

[26]-Thomas,S., & Pothan L.A, (2008). Natural Fibre Reinforced Polymer Composites: From Macro to Nanoscale, *Old City Publishing Inc.*

[27] Shumigin, D., Tarasova, E., Krumme, A., & Meier, P. (2011). Rheological and mechanical properties of poly (lactic) acid/cellulose and LDPE/cellulose composites. *Materials Science*, 17(1), 32-37.

[28] Haque, M., Rahman, R., Islam, N., Huque, M., & Hasan, M. (2010). Mechanical properties of polypropylene composites reinforced with chemically treated coir and abaca fiber. *Journal of Reinforced Plastics and Composites*, 29(15), 2253-2261.

[29] Pierson, H. O. (2012). Handbook of carbon, graphite, diamonds and fullerenes: processing, properties and applications. *William Andrew.*

[30] Mehmet,S. ,Yoldas,S.,Kutlay,S., &Durmuskahya,C. (2014). Determination of properties of Althaea officinalis L. (Marshmallow) fibres as a potential plant fibre in polymeric composite materials, *Composites: Part B* 57 180–186.

[31] Mohanty, S., Verma, S. K., & Nayak, S. K. (2006). Dynamic mechanical and thermal properties of MAPE treated jute/HDPE composites. *Composites Science and Technology*, 66(3-4), 538-547.

[32] Nagarajan, T. T., Babu, A. S., Palanivelu, K., & Nayak, S. K. (2016, March). Mechanical and Thermal Properties of PALF Reinforced Epoxy Composites. *In Macromolecular Symposia*(Vol. 361, No. 1, pp. 57-63).

[33] Arya Uthaman, Hiran Mayookh Lal, Chenggao Li, Guijun Xian, and Sabu Thomas (2021). Mechanical and Water Uptake Properties of Epoxy Nanocomposites with Surfactant-Modified Functionalized Multiwalled Carbon Nanotubes, *Nanomaterials (Basel).* 11(5): 1234.

[34] Tjong, S. C., Liang, G. D., & Bao, S. P. (2007). Electrical behavior of polypropylene/multiwalled carbon nanotube nanocomposites with low percolation threshold. *Scripta Materialia*, 57(6), 461.

[35]Bikiaris, D., Vassiliou, A., Chrissafis, K., Paraskevopoulos, K. M., Jannakoudakis, A., & Docoslis, A. (2008). Effect of acid treated multi-walled carbon nanotubes on the mechanical, permeability, thermal properties and thermo-oxidative stability of isotactic polypropylene. *Polymer Degradation and Stability*, 93(5), 952-967.

[36]Nurdina, A. K., Mariatti, M., & Samayamutthirian, P. (2009). Effect of single- mineral filler and hybrid-mineral filler additives on the properties of polypropylene composites. *Journal of Vinyl and Additive Technology*, 15(1), 20-28.

[37] Lux, F. (1993). Models proposed to explain the electrical conductivity of mixtures made of conductive and insulating materials. *Journal of materials science*, 28(2), 285-301.

[38]-He, D., & Jiang, B. (1993). The elastic modulus of filled polymer composites. *Journal of applied polymer science*, 49(4), 617-621.

[39] Lee, S. H., Cho, E., Jeon, S. H., & Youn, J. R. (2007). Rheological and electrical properties of polypropylene composites containing functionalized multi-walled carbon nanotubes and compatibilizers. *Carbon*, 45(14), 2810-2822.